Catalysis Today 149 (2010) 191–195

Contents lists available at ScienceDirect

Catalysis Today

journal homepage: www.elsevier.com/locate/cattod

Temperature profile in a two-stage fixed bed reactor for catalytic partial oxidation of methane to syngas

Jian Xu [a,b,*], Weisheng Wei [b], Aizhen Tian [b], Yu Fan [a,b], Xiaojun Bao [a,b], Changchun Yu [b]

[a] The State Key Laboratory of Heavy Oil, China University of Petroleum, Beijing 102249, China
[b] The Key Laboratory of Catalysis, China National Petroleum Co., China University of Petroleum, Beijing 102249, China

ARTICLE INFO

Article history:
Available online 14 August 2009

Keywords:
Partial oxidation of methane
Fixed bed reactor
Two-stage process
Multiple oxygen feeding

ABSTRACT

Detailed axial temperature distribution has been studied in a two-stage process for catalytic partial oxidation of methane to syngas, which consists of two consecutive fixed bed reactors with oxygen or air separately introduced. The first stage of the reactor, packed with a combustion catalyst, is used for catalytic combustion of methane at low initial temperature. While the second stage, filled with a partial oxidation catalyst, is used for the partial oxidation of methane to syngas. A pilot-scale reactor packed with up to 80 g combustion catalyst and 80 g partial oxidation catalyst was employed. The effects of oxygen distribution in the two sections, and gas hourly space velocity (*GHSV*) on the catalyst bed temperature profile, as well as conversion of methane and selectivities to syngas were investigated under atmospheric pressure. It is found that both oxygen splitting ratio and *GHSV* have significant influence on the temperature profile in the reactor, which can be explained by the synergetic effects of the fast exothermic oxidation reactions and the slow endothermic (steam and CO_2) reforming reactions. Almost no change in activity and selectivity was observed after a stability experiment for 300 h.

1. Introduction

Large deposits of natural gas, rising crude oil price, growing importance of environmental protection have stimulated numerous global R&D efforts for converting natural gas into more valuable chemical feed stocks and liquid fuels. In addition, remote locations of much of the discovered gas reserves make it desirable to convert the gas on-site to liquid products that are economically transportable [1–5]. Syngas production is an important intermediate step in the gas to liquid (GTL) processes, which is roughly responsible for about 60–70% of the total cost [1]. Reducing the cost of syngas production would have great beneficial effects on the overall economics of GTL process [6–10].

The dominated commercial method to produce syngas is steam reforming of methane via:

$$CH_4 + H_2O \rightarrow CO + 3H_2 \qquad \Delta H_{298\,K} = 205.9\,kJ/mol \qquad (1)$$

because of its high endothermicity and production at a 3:1 H_2:CO ratio, this process is characterized by high investment costs and energy consumption [11].

An alternative syngas production process that has received extensive attention is the catalytic partial oxidation of methane to syngas.

$$CH_4 + 0.5O_2 \rightarrow CO + 2H_2 \qquad \Delta H_{298\,K} = -35.6\,kJ/mol \qquad (2)$$

since its mild exothermicity, this process would be much energy efficient than the energy intensive steam reforming process. It also gives the desired 2:1 H_2:CO ratio required for downstream conversion by Fischer–Tropsch synthesis or methanol synthesis. Furthermore, the residence time of catalytic partial oxidation is on the order of a few milliseconds, which is much faster than steam reforming (the residence time is on the order of 0.5–1 s). Thus for the same production capacity, syngas facilities for the partial oxidation of methane can be far smaller, and less expensive, than facilities based on steam reforming.

Intensive research efforts on catalytic partial oxidation of methane to syngas have been carried out, concentrating on both catalyst development and reaction engineering [12–17]. However, this technology has not yet been applied at an industrial scale [3]. Many scientific and engineering challenges remain to be solved before commercialization of the catalytic partial oxidation of methane to syngas can be implemented. One of the major engineering problems is the formation of high temperature gradient (hot spot) in catalyst bed which gives rise to catalyst melting and deactivation [13,15,18,19]. It is widely accepted that

* Corresponding author at: P.O. Box 277, China University of Petroleum, Changping, Beijing 102249, China. Tel.: +86 10 89734981; fax: +86 10 89734979.
E-mail address: xujian@cup.edu.cn (J. Xu).

0920-5861/$ – see front matter © 2009 Elsevier B.V. All rights reserved.
doi:10.1016/j.cattod.2009.07.087

catalytic partial oxidation of methane occurs in a two-step mechanism. Methane is firstly total oxidized (Eq. (3)) to CO_2 and water in the first part of the catalyst bed until oxygen is exhausted, followed by reforming of the remaining methane with the CO_2 and water formed initially (Eqs. (1) and (4)). Therefore, a sharp temperature profile over the reactor will always be present because total oxidation is strongly exothermic whereas the reforming reactions are endothermic. Another major engineering problem is the formation of potentially explosive mixture when the reactant methane and oxygen would be premixed [13,15].

$$CH_4 + 2O_2 \rightarrow CO_2 + 2H_2O \qquad \Delta H_{298\,K} = -802\,kJ/mol \tag{3}$$

$$CH_4 + CO_2 \rightarrow 2CO + 2H_2 \qquad \Delta H_{298\,K} = 247\,kJ/mol \tag{4}$$

Temperature gradients can be minimized using a fluidized bed reactor [20,21] or a spouted bed reactor [22,23], both provide good heat integration. Another way to minimize the temperature gradients is by various reactor designs for coupling exothermic oxidation reactions and endothermic reforming reactions, which can be classified into recuperative coupling, regenerative coupling and direct coupling [24–27].

Attentions have also been paid to the risk of explosion with premixed CH_4 and O_2. High risks of explosion are expected to be encountered under industrial operating conditions due to high temperatures and pressures. Apparatus and process to provide complete and rapid mixture of methane and oxygen were proposed, so that these two reactants can be fully mixed and safely delivered to the catalytic reaction zone before homogeneous reaction is initiated [28,29].

Another way to overcome the possible formation of explosive mixtures and flatten the temperature gradients is distributive supply of oxygen to the catalytic reaction zone [30–32]. Smit et al. [31] used a porous membrane in a reverse flow reactor to distributively feed the oxygen. A flat temperature plateau without any hot spots was observed, demonstrating the advantage of distributive feeding of oxygen. Barrio et al. [32] used a one-dimensional quasi-homogeneous reactor model to study potentials for optimization of a catalytic partial oxidation process with Ru catalyst in a fixed bed reactor. The results showed that split of oxygen along the reactor allowed a noticeable decrease of the maximum temperature in the reactor.

Based on the two-step mechanism, alternative catalyst bed configurations, such as dual bed or mixed catalyst bed reactors have also been examined. Zhu et al. [33] demonstrated a dual catalyst bed system taking advantages of both stability of oxide catalyst and good activity of metal catalyst. An oxide catalyst was used in the first catalyst bed to carry out partial oxidation with 100% oxygen conversion. A metal catalyst was used in the second catalyst bed to convert the unconverted methane to syngas by steam and CO_2 reforming reactions. Tong et al. [34] proposed a sequential bed catalyst made up of a platinum coated monolith for combustion followed immediately by a nickel coated monolith for reforming to produce syngas.

It should be noted that many studies on process development and reactor design for catalytic partial oxidation of methane to syngas were based on either numerical simulation by using reactor models, or experimental works in micro-scale reactors [32,35–42]. Experimental results in a pilot-scale reactor system are therefore of great importance.

In previous contributions, a two-stage partial oxidation process which consists of two consecutive fixed bed reactors with separately introduced oxygen or air was proposed [43]. The first reactor, which was packed with a perovskite type oxide catalyst, was used for the catalytic combustion of methane at a low initial temperature (623–673 K). The second reactor, which was filled with a partial oxidation catalyst such as a Ni-based catalyst, was used for the partial oxidation of methane to syngas. A portion of methane was oxidized to CO_2 and H_2O in the first reactor, in which the reactants were simultaneously heated to the temperature required for methane partial oxidation (>1073 K). The remaining oxygen was introduced between the exit of first reactor and the inlet of second reactor. In the second reactor, exothermic partial oxidation of methane and endothermic reforming reactions of CO_2 and H_2O occurred to produce syngas. By splitting the oxygen feed, the mixture of methane and oxygen was not within the explosion limit in either reactor. Preliminary experimental studies with 5 g catalysts in both of the two reactors showed that the two-stage reactor had advantages in reducing the possibility and magnitude of hot spots created during the catalytic oxidations of methane, while allowing safer operation [43].

In the present study, in order to further scale-up this process, a pilot-scale two-stage fixed bed reactor was established, which can be filled with up to 80 g catalyst in both stages. Detail temperature profiles in catalyst beds were investigated under various operating conditions. The effects of oxygen splitting ratio in the two sections, and gas hourly space velocity on the catalyst bed temperature distribution, as well as conversion of methane and selectivity to syngas were experimentally studied.

2. Experimental

2.1. Apparatus

A schematic of the pilot-scale two-stage fixed bed reactor operating at atmosphere pressure is shown in Fig. 1. The reactor consists of a stainless steel tube of 1.5 m in length and 25 mm in inner diameter. The first stage of the reactor (combustion section) is filled with 15–80 g lanthanum-based perovskite type oxide catalyst, while the second stage of the reactor (oxidation and reforming section) is filled with 15–80 g La_2O_3 promoted Ni/$MgAl_2O_4$–Al_2O_3 catalyst. A layer of ceramic ring is filled before and after each of the two catalyst layers, serving as heat shield for the catalyst beds and flow distributor for reactant gases. A 6 mm ID stainless steel tube for feeding the remaining oxygen is sealed on one end and inserted into the ceramic ring layer between the two catalyst layers. There are several 2 mm diameter holes along the tube, facilitating better mixing of the oxygen with effluent gases (CO_2, H_2O and unconverted CH_4) from the combustion section before entering into the oxidation and reforming section.

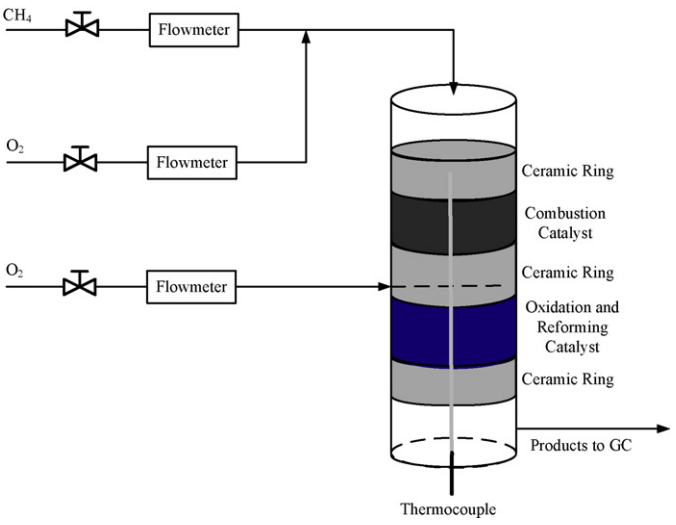

Fig. 1. A schematic of the two-stage fixed bed reactor for catalytic partial oxidation of methane to syngas.

Three electric ovens, whose temperature can be controlled and fine-tuned, are placed outside the reactor to preheat the reactant mixture and the catalyst beds. A thermowell (stainless steel, outer diameter: 3 mm) equipped with a movable thermocouple is placed in the center of the catalyst bed in order to monitor the temperature profile along the reactor. The feed and products were analyzed on an on-line gas chromatograph equipped with a Porapak N column and a 5A Molecular Sieve column using TCD detector.

2.2. Catalysts preparation

2.2.1. Catalyst for combustion of methane

A supported La-based perovskite type oxide catalyst $La_{0.7}Ca_{0.3}Fe_{0.3}Mn_{0.7}O_3$ (LCFM) is prepared by impregnation of γ-Al_2O_3 support (from Condea, γ-Al_2O_3 spheres of 2–3 mm diameter) with a citric acid complex solution having given amounts of La, Ca, Fe and Mn ions. The catalyst is then dried and calcined at 1073 K for 6 h.

2.2.2. Catalyst for partial oxidation of methane

A La_2O_3 promoted 7 wt.% Ni/$MgAl_2O_4$–Al_2O_3 catalyst (atomic ratio of Ni/La/Mg = 100/63/63) is prepared by a two-step impregnation process. First, the γ-Al_2O_3 support is impregnated with an aqueous solution of magnesium nitrate, dried at 633 K and calcined at 1173 K for 10 h to form $MgAl_2O_4$ spinel compound on the surface of γ-Al_2O_3; second, the $MgAl_2O_4$–Al_2O_3 is impregnated with a mixed aqueous solution of nickel nitrate and lanthanum nitrate, then dried at 363 K and calcined at 973 K for 6 h.

2.3. Reactor performance

Reactor performance is quantized by the conversion of reactants and selectivities to desired products. The conversion of species i (X_i) is calculated as the ratio of the reactant consumed to that fed:

$$X_i = \frac{F_{i,in} - F_{i,out}}{F_{i,in}} \quad (5)$$

where $F_{i,in}$ is the flow rate of species i into the reactor and $F_{i,out}$ is the flow of species i leaving the reactor, both corrected to standard conditions (T = 298 K, P = 1 atm).

The selectivity of atom i to form species j ($S_{i,j}$) is defined as:

$$S_{i,j} = \frac{\nu_{i,j}F_{i,out}}{\sum_k \nu_{i,k}F_{k,out}} \quad (6)$$

where $\nu_{i,j}$ is the stoichiometric amount of atom i in species j. The denominator is the sum over all species, k. The yield of a product is the conversion multiplied by the product selectivity.

The gas hourly space velocity (*GHSV*) is calculated from the volumetric flow rate at standard conditions divided by the void volume of the catalyst:

$$GHSV = \frac{V_{total}}{\varepsilon V_{catalyst}} \quad (7)$$

where V_{total} is the volumetric flow rate at standard conditions, ε is the void fraction of catalyst bed, and $V_{catalyst}$ is the volume of the catalyst bed.

3. Results and discussion

3.1. Effect of oxygen feed distribution

Effect of oxygen distribution on temperature profiles in both catalyst beds and on conversion of methane and selectivities to CO and H_2 was investigated in the two-stage reactor filled with 15 g combustion catalyst and 15 g partial oxidation catalyst. Both catalyst beds have a length of about 38 mm. Fig. 2 shows temperature profiles along the centerline axis of catalyst beds at three different oxygen splitting ratios while the overall ratio of feed CH_4 to O_2 is kept at 2:1. The reactant gas and the two catalyst beds are preheated to 623, 773 and 973 K, respectively. It can be seen from Fig. 2 that the combustion catalyst bed experiences a significant temperature rise at the initial portion of the bed. Furthermore, the peak temperature dramatically increases as the increase of oxygen content in the feed of the first stage. For the operations with feed ratio of CH_4:O_2 (first feed):O_2 (second feed) = 8:1:3, 8:2:2, and 8:3:1, the peak temperature are 929, 1091 and 1252 K, respectively. Such a high temperature at the entrance of the reactor is undesirable due to the ignition of unexpected homogeneous gas phase reaction [16,44]. On the other hand, the temperature profile along the oxidation reforming catalyst bed is much flattened, although a peak temperature still exists. The largest temperature difference for the three cases is less than 50 K. Higher content of oxygen in the feed of the second stage gives rise to higher exit bed temperature, and accordingly higher overall conversion of methane and selectivity to syngas, as depicted in Table 1. Oxygen conversion is complete for all the cases. The equilibrium methane conversion and selectivity to CO calculated according to the exit bed temperature for each case are also given in Table 1. The large deviation between the experimental result and the equilibrium value can be explained by the high gas space velocity employed, which will be discussed in detail in next section.

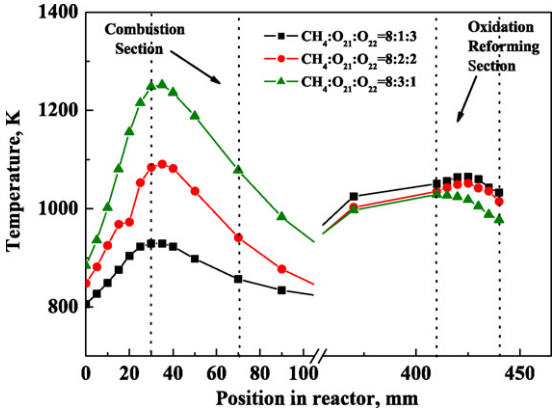

Fig. 2. Temperature profiles along the centerline axis of catalyst beds at different oxygen splitting ratio, *GHSV* = 10,000 h^{-1}, combustion catalyst: 15 g, partial oxidation catalyst: 15 g.

Experiments are also conducted at the reactor with more catalysts filled (80 g, about 160 mm in length for each catalyst) and with much lower gas space velocity (*GHSV* = 2500 h^{-1}), at different oxygen splitting ratios. The temperature profiles of the catalyst beds are shown in Fig. 3 and the conversion of methane and selectivities to syngas are given in Table 2. Similar results can be seen as those shown in Fig. 2 and Table 1. However, much higher methane conversion and syngas selectivities are achieved, which are close to thermodynamic equilibrium. This can also be explained by a longer reactant catalyst contact time due to a much lower gas space velocity employed, which will be discussed in the next section.

It can be seen from Fig. 3 and Table 2 that a much flattened temperature profile in the combustion catalyst bed and a relatively higher methane conversion and syngas selectivity are achieved with a feed ratio of CH_4:O_2 (first feed):O_2 (second feed) = 8:0.5:3.5. However, such an oxygen splitting ratio may go beyond the original intention of this process concept to avoid possible

Table 1
Conversion of methane and selectivity to CO at different oxygen splitting ratio, *GHSV* = 10,000 h^{-1}, overall CH_4:O_2 = 2:1, combustion catalyst: 15 g, partial oxidation catalyst: 15 g.

CH_4:O_{21}:O_{22}	X_{CH_4} (%)		S_{CO} (%)	
	Experiment	Equilibrium	Experiment	Equilibrium
8:1:3	72.6	88.6	85.4	95.2
8:2:2	64.4	85.8	78.7	93.6
8:3:1	54.4	79.8	65.1	89.4

Table 2
Conversion of methane and selectivity to CO and H_2 at different oxygen splitting ratio, *GHSV* = 2500 h^{-1}, overall CH_4:O_2 = 2:1, combustion catalyst: 80 g, partial oxidation catalyst: 80 g.

CH_4:O_{21}:O_{22}	X_{CH_4} (%)	X_{O_2} (%)	S_{CO} (%)	S_{H_2} (%)
8:1:3	93.2	100.0	99.0	97.4
8:0.5:3.5	94.4	100.0	99.2	97.9

explosion by reducing oxygen content in the feeding reactant gas. Further study is necessary to determine an optimum oxygen distribution. A feed ratio of CH_4:O_2 (first feed):O_2 (second feed) = 8:1:3 is fixed in the following experiments.

It is well accepted that oxidation reactions and reforming reactions appear to occur with different predominance over the length of a catalytic partial oxidation packed bed reactor. Exothermic oxidation reactions tend to predominate in the initial part of the catalyst bed, whereas endothermic reforming reactions predominate in the downstream portion. Thus, the temperature rise in the combustion section needs to be controlled by minimum consumption of methane. While a sustained and high enough temperature however is preferred for the second stage to carry out the predominantly reforming reactions to near completion. Therefore, it can be concluded that relatively higher oxygen content in the second stage is necessitated in order to obtain a flat temperature profile and high methane conversion and syngas selectivity.

3.2. Effect of gas space velocity (GHSV)

Figs. 4 and 5 show experimental results obtained with the reactor packed with 60 g combustion catalyst and 60 g partial oxidation catalyst, respectively. Temperature profile in the catalyst beds, conversion of CH_4, and selectivities to CO and H_2 are shown as a function of *GHSV*.

It can be shown from Fig. 4 that gas space velocity has a pronounced influence on the temperature distribution in both the combustion and the partial oxidation catalyst beds. As *GHSV* rises, from 2500 to 10,000 h^{-1}, the peak temperature in the catalyst bed increases dramatically due to the increase of thermal energy produced for a unit time period. The peak temperatures in the combustion catalyst bed for all the *GHSV* investigated are all at the front of the bed, after which the temperature decreases gradually. However, the temperature profile along the second stage of the reactor evolves differently for relatively higher and relatively lower space velocity. When the space velocity is high (≥5000 h^{-1}), a peak temperature appears at the front of the catalyst bed. The temperature is then decreased gradually along the bed. While for a lower space velocity (<5000 h^{-1}), an obvious minimum temperature appears after the peak temperature, followed by further temperature increase in the posterior catalyst bed.

In the second stage of the reactor, the remaining methane from first stage, together with H_2O and CO_2 which are produced from methane combustion in the first stage, and with the secondary feeding of oxygen, undergo exothermic oxidation reactions and strongly endothermic steam and/or CO_2 reforming reactions at the present of partial oxidation catalyst. The oxidation reaction rate is much faster than that of reforming reaction. A study by Vermeiren et al. [45] with 5 wt.% Ni catalyst showed that the rate of partial oxidation reaction is 13 times faster than that of steam reforming reaction. Therefore, the minimum temperature appears in the catalyst bed after a peak temperature (indicating occurrence of oxidation reactions) at relatively lower space velocity can be explained by complete reforming reactions due to sufficient gas catalyst contact time. This can be further confirmed by the effect of gas space velocity on methane conversion and syngas selectivity as shown in Fig. 5. The conversion of methane and the selectivities to CO and H_2 are all decreased as the increase of gas space velocity, indicating incomplete reforming reactions.

It also can be seen that, at lower gas space velocity, both the conversion of methane and the selectivity to CO first increase then decrease with the increase of gas space velocity. Maximum values are obtained when *GHSV* reaches around 2500 h^{-1}. This can be explained by the synergetic effect of gas space velocity on heat effect of the reactor and the contact time between reactant and catalyst. A lower gas space means less reaction heat released for a certain period of time, hence lower temperature the catalyst bed can be maintained at, and accordingly decreased methane conversion and syngas selectivity. On the contrast, a higher bed temperature can be sustained at a higher space velocity, but may be subject to insufficient gas–catalyst contact.

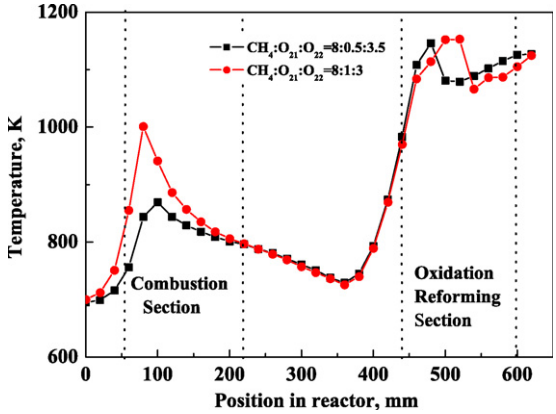

Fig. 3. Temperature profiles along the centerline axis of catalyst beds at different oxygen splitting ratio, *GHSV* = 2500 h^{-1}, combustion catalyst: 80 g, partial oxidation catalyst: 80 g.

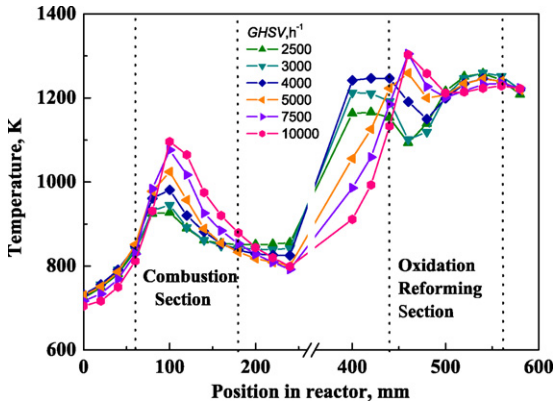

Fig. 4. Effect of gas space velocity on temperature profile in catalyst beds, CH_4:O_2 (first feed):O_2 (second feed) = 8:1:3, combustion catalyst: 60 g, partial oxidation catalyst: 60 g.

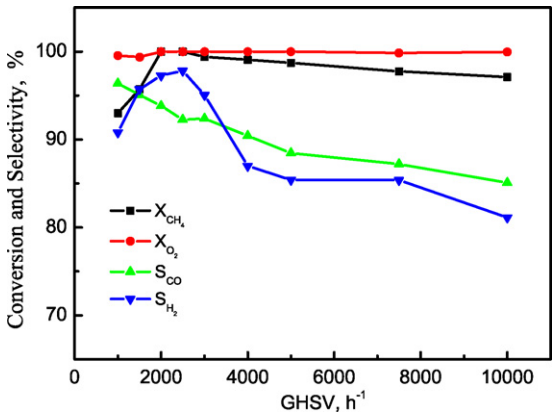

Fig. 5. Effect of gas space velocity on conversion of methane and selectivity to syngas, CH_4:O_2 (first feed):O_2 (second feed) = 8:1:3, combustion catalyst: 60 g, partial oxidation catalyst: 60 g.

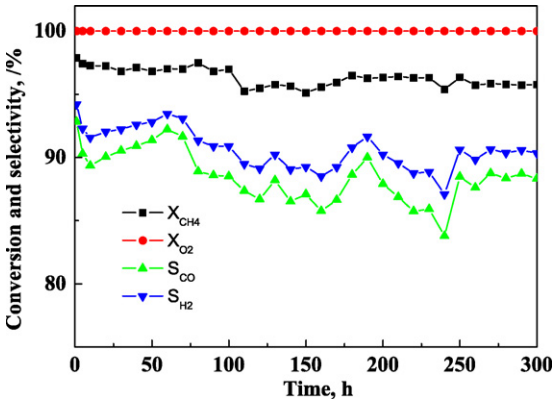

Fig. 6. Results from stability experiment, CH_4:O_2 (first feed):O_2 (second feed) = 8:1:3, *GHSV* = 2000 h^{-1}, combustion catalyst: 80 g, partial oxidation catalyst: 80 g.

3.3. Stability experiment

It was argued that decreased O_2/CH_4 ratio in the reactant gas due to multiple oxygen addition would make carbon deposition thermodynamically more favorable and thus lead to deactivation of the catalyst [46]. A stability experiment has been carried out in the present study, the results are shown in Fig. 6. A CH_4 conversion of about 95% and selectivities to CO and H_2 of about 95% were achieved at a feed ratio of feed ratio of CH_4:O_2 (first feed):O_2 (second feed) = 8:1:3, and a *GHSV* of 2000 h^{-1}. Almost no changes in activity and selectivity were observed after 300 h of operation. This is consistent with thermodynamic calculations [47], that both a high temperature prevailing in the first stage and relative high oxygen content in the feed of the second stage suppress the carbon deposition thermodynamically.

4. Conclusion

Both oxygen distribution in the two stages and *GHSV* have significant influences on the temperature profile in the reactor, and conversion of methane and selectivities to syngas. Relatively higher oxygen content in the second stage is necessitated in order to obtain a flat temperature profile and high methane conversion and syngas selectivity. When the space velocity is high ($\geq$5000 h^{-1}), a peak temperature appears at the front of the catalyst bed. The temperature is then decreased gradually along the bed. While for a lower space velocity (<5000 h^{-1}), an obvious minimum temperature appears after the peak temperature, followed by further temperature increase in the posterior catalyst bed. This can be explained by the synergetic effects of fast exothermic oxidation reactions and slow endothermic (steam and CO_2) reforming reactions. A stability experiment has been carried out for 300 h, no obvious changes in activity or selectivity were observed, indicating the reliability of the two-stage process.

Acknowledgements

Financial support by the China National Natural Science Foundation programs (Grant Nos. 20490200 and 20776156) is gratefully acknowledged.

References

[1] K. Aasberg-Petersen, J.H. Bak Hansen, T.S. Christensen, I. Dybkjaer, P.S. Christensen, C. Stub Nielsen, S.E.L. Winter Madsen, J.R. Rostrup-Nielsen, Applied Catalysis A: General 221 (2001) 379.
[2] M.E. Dry, Catalysis Today 71 (2002) 227.
[3] P. Ferreira-Aparicio, M.J. Benito, J.L. Sanz, Catalysis Reviews 47 (2005) 491.
[4] D.J. Wilhelm, D.R. Simbeck, A.D. Karp, R.L. Dickenson, Fuel Processing Technology 71 (2001) 139.
[5] J.R. Rostrup-Nielsen, Catalysis Today 71 (2002) 243.
[6] M.A. Pena, J.P. Gomez, J.L.G. Fierro, Applied Catalysis A: General 144 (1996) 7.
[7] J.R. Rostrup-Nielsen, Catalysis Today 63 (2000) 159.
[8] L. Basini, Catalysis Today 106 (2005) 34.
[9] A.C. Vosloo, Fuel Processing Technology 71 (2001) 149.
[10] F. Yagi, R. Kanai, S. Wakamatsu, R. Kajiyama, Y. Suehiro, M. Shimura, Catalysis Today 104 (2005) 2.
[11] J.R. Rostrup-Nielsen, Catalytic Steam Reforming, Springer-Verlag, 1984.
[12] A.P.E. York, T. Xiao, M.L.H. Green, Topics in Catalysis 22 (2003) 345.
[13] Y.H. Hu, E. Ruckenstein, Advances in Catalysis 48 (2004) 297.
[14] A.P.E. York, T.-c. Xiao, M.L.H. Green, J.B. Claridge, Catalysis Reviews 49 (2007) 511.
[15] B.C. Enger, R. Løeng, A. Holmen, Applied Catalysis A: General 346 (2008) 1.
[16] M.F. Reyniers, C.R.H. de Smet, P.G. Menon, G.B. Marin, CATTECH 6 (2002) 140.
[17] T. Liu, C. Snyder, G. Veser, Industrial & Engineering Chemistry Research 46 (2007) 9045.
[18] B. Li, S. Kado, Y. Mukainakano, M. Nurunnabi, T. Miyao, S. Naito, K. Kunimori, K. Tomishige, Applied Catalysis A: General 304 (2006) 62.
[19] F. Basile, G. Fornasari, F. Trifiro, A. Vaccari, Catalysis Today 64 (2001) 21.
[20] K. Tomishige, Y. Matsuo, Y. Yoshinaga, Y. Sekine, M. Asadullah, K. Fujimoto, Applied Catalysis A: General 223 (2002) 225.
[21] M.E.E. Abashar, International Journal of Hydrogen Energy 29 (2004) 799.
[22] K.G. Marnasidou, S.S. Voutetakis, G.J. Tjatjopoulos, I.A. Vasalos, Chemical Engineering Science 54 (1999) 3691.
[23] W. Wei, J. Xu, D. Fang, X. Bao, Chinese Journal of Chemical Engineering 11 (2003) 643.
[24] J. Frauhammer, G. Eigenberger, L.v. Hippel, D. Arntz, Chemical Engineering Science 54 (1999) 3661.
[25] G. Kolios, J. Frauhammer, G. Eigenberger, Chemical Engineering Science 57 (2002) 1505.
[26] R.C. Ramaswamy, P.A. Ramachandran, M.P. Dudukovic, Chemical Engineering Science 61 (2006) 459.
[27] R.C. Ramaswamy, P.A. Ramachandran, M.P. Dudukovic, Chemical Engineering Science 63 (2008) 1654.
[28] US Patent, Application Number 7,108,838.
[29] US Patent, Application Number 6,471,937.
[30] G. Veser, J. Frauhammer, U. Friedle, Catalysis Today 61 (2000) 55.
[31] J. Smit, G.J. Bekink, M. van Sint Annaland, J. Kuipers, International Journal of Chemical Reactor Engineering 3 (2005) A12.
[32] V.L. Barrio, G. Schaub, M. Rohde, S. Rabe, F. Vogel, J.F. Cambra, P.L. Arias, M.B. Guemez, International Journal of Hydrogen Energy 32 (2007) 1421.
[33] J. Zhu, M.S.M.M. Rahuman, J.G. van Ommen, L. Lefferts, Applied Catalysis A: General 259 (2004) 95.
[34] G.C.M. Tong, J. Flynn, C.A. Leclerc, Catalysis Letters 102 (2005) 131.
[35] M.E.E. Abashar, S. Elnashaie, Chemical Engineering Research and Design 85 (2007) 1529.
[36] D.G. Vlachos, A.B. Mhadeshwar, N.S. Kaisare, Computers & Chemical Engineering 30 (2006) 1712.
[37] G.A. Viswanathan, D. Luss, AIChE Journal 52 (2006) 1533.
[38] R. Quiceno, J. Perez-Ramirez, J. Warnatz, O. Deutschmann, Applied Catalysis A: General 303 (2006) 166.
[39] S.H. Chan, D.L. Hoang, O.L. Ding, International Journal of Heat and Mass Transfer 48 (2005) 4205.
[40] M. Bizzi, G. Saracco, R. Schwiedernoch, O. Deutschmann, AIChE Journal 50 (2004) 1289.
[41] M. Bizzi, L. Basini, G. Saracco, V. Specchia, Industrial & Engineering Chemistry Research 42 (2003) 62.
[42] P.M. Biesheuvel, G.J. Kramer, AIChE Journal 49 (2003) 1827.
[43] S. Shen, Z. Pan, C. Dong, Q. Jiang, Z. Zhang, C. Yu, in: E. Iglesia, J.J. Spivey, T.H. Fleisch (Eds.), Studies in surface science and catalysis, 136, Elsevier, 2001, p. 99.
[44] P.O. Thevenin, P.G. Menon, S.G. Järås, CATTECH 7 (2003) 10.
[45] W.J.M. Vermeiren, E. Blomsma, P.A. Jacobs, Catalysis Today 13 (1992) 427.
[46] H. Papp, P. Schuler, Q. Zhuang, Topics in Catalysis 3 (1996) 299.
[47] J. Xu, W. Wei, X. Bao, Chinese Journal of Chemical Engineering 10 (2002) 56.